

LETTER TO THE EDITOR

First detection of hydrogen isocyanide (HNC) in Titan's atmosphere

R. Moreno¹, E. Lellouch¹, L. M. Lara², R. Courtin¹, D. Bockelée-Morvan¹, P. Hartogh³,
M. Rengel³, N. Biver¹, M. Banaszekiewicz⁴, and A. González^{3,2}

¹ LESIA – Observatoire de Paris, CNRS, Université Paris 06, Université Paris–Diderot, 5 place Jules Janssen, 92195 Meudon, France
e-mail: raphael.moreno@obspm.fr

² Instituto de Astrofísica de Andalucía (CSIC), Granada, Spain

³ Max-Planck-Institut für Sonnensystemforschung, Katlenburg-Lindau, Germany

⁴ Space Research Centre of Polish Academy of Sciences, Warsaw, Poland

Received 30 September 2011 / Accepted 22 November 2011

ABSTRACT

We report on the first identification of hydrogen isocyanide (HNC) in Titan's atmosphere, from observations using the HIFI instrument on the *Herschel** Space Observatory. An emission line from the HNC $J = 6 \rightarrow 5$ rotational transition at 543.897 GHz was measured in Titan on June 14 and December 31, 2010. Radiative transfer modeling indicates that the bulk of HNC is located above 400 km, with a column density in the range $(0.6\text{--}1.5) \times 10^{13} \text{ cm}^{-2}$, but the observations cannot establish its vertical profile. In particular HNC could be restricted to the upper thermosphere (~ 1000 km), in which case its local abundance relative to HCN could be as high as ~ 0.3 . HNC is probably formed mostly at ionospheric levels (950–1150 km) from dissociative recombination of HCNH^+ and possibly other heavier nitrile ions. Ionospheric loss of HNC occurs by protonation with XH^+ ions. Additional formation (e.g. from $\text{N}(^4\text{S}) + ^3\text{CH}_2$) and loss routes (e.g. from isomerization to HCN) in the neutral atmosphere remain to be investigated.

Key words. techniques: spectroscopic – submillimeter: planetary systems – planets and satellites: individual: Titan

1. Introduction

Titan is the only satellite of the Solar System to possess a dense atmosphere (1.5 bar), mainly composed of N_2 with a few percent of CH_4 . The detection of hydrogen cyanide (HCN) and of more complex nitriles (HC_3N and C_2N_2) obtained by IR spectrometers onboard spacecrafts (starting with Voyager in 1980) was of considerable interest, as these molecules are key intermediates in the synthesis of organic molecules. Their presence, along with that of several hydrocarbons, implies a complex photochemistry of methane, which is, on the one hand, coupled with that of N_2 , and on the other hand, enriched by ion-molecule reactions taking place in the upper atmosphere (>800 km). As a matter of fact, and as one of the major discoveries of the Cassini mission at Titan, numerous heavy organic molecules have been detected in Titan's upper atmosphere by Cassini Ion Neutral Mass Spectrometer (INMS), (e.g. Waite et al. 2005; Vuitton et al. 2007). Despite these impressive results, from which a completely new view of Titan's ion-neutral chemistry emerged, INMS cannot distinguish between species of identical mass, in particular between isomers. Heterodyne spectroscopy of strong rotational lines provides high sensitivity and frequency discrimination for the detection of minor species with permanent dipole moment – such as HCN, HC_3N and CH_3CN (Marten et al. 2002; Gurwell 2004), and CO (Gurwell & Muhleman 1995; Hidayat et al. 1998; Rengel et al. 2011) – and allows for full resolution of line profiles, as well as unique absolute wind measurements in Titan's stratosphere and mesosphere from mapping of the Doppler shift in spatially-resolved data (Moreno et al. 2005).

In this paper, we report the first detection of a new species, hydrogen isocyanide (HNC), in Titan's atmosphere, using the Heterodyne Instrument for the Far-Infrared (HIFI, de Graauw et al. 2010) onboard the ESA *Herschel* Space Observatory (Pilbratt et al. 2010).

2. Observations

Observations of Titan were performed on June 14 and December 31, 2010, as part of the *Herschel* guaranteed time key program “Water and related chemistry in the Solar System” (HssO, see Hartogh et al. 2009). We used the HIFI heterodyne receiver in band 1a (covering the 480–560 GHz spectral region), with two orthogonal polarizations (H and V) simultaneously.

The original goal of these observations was to study water vapor in Titan's atmosphere. The receiver was therefore tuned to the $\text{H}_2\text{O}(1_{10}\text{--}1_{01})$ rotational transition at 556.936 GHz, in the upper sideband (USB). In June 2010, the local oscillator (LO) frequency of the instrument was tuned to 550.390 GHz. Because HIFI is a double sideband (DSB) receiver, its lower sideband (LSB) simultaneously covered the 542.4–546.4 GHz range. For spectral analysis, we used two different spectrometers at a spectral resolution of 1.1 MHz (Wide Band Spectrometer, WBS) and 0.25 MHz (High Resolution Spectrometer, HRS). The telescope half power beam width (HPBW) at 556 GHz is $39''$. To minimize the contribution from Saturn, Titan was observed at eastern elongation ($173''$ east of Saturn) using a position switch (PSw) observing mode. The reference sky position was chosen to be separated from Titan by $+2'$ in declination (i.e. North of Titan) in order to avoid any contamination from Saturn. Data reduction was carried out using the *Herschel* data reduction software (HIPE, Ott 2010), which calibrates the data flux and corrects for spacecraft and planet velocity. A polynomial baseline removal was performed to eliminate the standing waves.

* *Herschel* is an ESA space observatory with science instruments provided by European-led Principal Investigator consortia and with important participation from NASA.

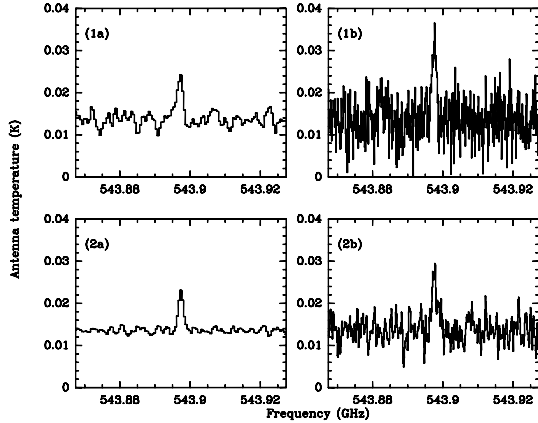


Fig. 1. Observations of HNC(6–5) at 543.897 GHz on Titan measured with *Herschel*/HIFI. Both H and V polarizations are averaged. **1a)** Upper left panel: measurement with WBS ($\Delta\nu = 1.1$ MHz) on June 14, 2010. **1b)** Upper right panel: measurement with HRS ($\Delta\nu = 0.25$ MHz) on June 14, 2010. **2a)** Lower left panel: measurement with WBS on Dec. 31, 2010. **2b)** Lower right panel: measurement with HRS on Dec. 31, 2010. Due to varying distance of Titan, observations on Dec. 31 are scaled in intensity to the conditions of June 14.

Table 1. Summary of HIFI observations of Titan.

UT start date [yyyy mm dd.ddd]	Integration time [h]	Obs. mode	Δ [AU]	θ [$''$]
2010 06 14.822	4.54	PSw	9.390	0.756
2010 12 31.321	3.62	FSw	9.661	0.735

Notes. Δ is the distance between Titan and *Herschel*. θ is the surface apparent diameter. Observing modes are described in the text.

In addition to the water line (which will be reported separately), we unexpectedly detected in the LSB a narrow emission line at 543.897 GHz (Fig. 1), which we identified as the HNC(6–5) transition, representing the first detection of HNC in Titan’s atmosphere. To confirm the detection, additional observations of Titan were obtained on December 31, 2010, this time at western elongation. To increase the signal-to-noise ratio (S/N), instead of position switch we used the standard frequency switch (FSw) observing mode, with a frequency throw of 94.5 MHz. To confirm that the line was indeed from HNC(6–5), we used a slightly different tuning, 1 changing the LO frequency to 550.325 GHz. The line was again unambiguously detected, separately on each of the two spectrometers (Fig. 1) at the frequency of HNC(6–5). For both observational epochs, the HNC emission is narrow ($FWHM \sim 0.8$ km s $^{-1}$, or 1.5 MHz). The apparent diameter of Titan on December 31 was $\sim 6\%$ smaller than on June 14 (Table 1). After scaling the HNC line intensity to the June 14 conditions (Fig. 1), the line intensity ratio between the two epochs (June/Dec.) is 1.02 ± 0.10 implying no significant intensity variation over this time period or between the leading and trailing sides.

3. Modeling

The HNC spectra were analyzed with a line-by-line radiative transfer code accounting for the spherical geometry of Titan’s atmosphere (Marten et al. 2002, and references therein). This model considers HNC molecular opacities from the JPL catalog (Pickett et al. 1998), and also includes collision-induced opacities of N $_2$ –N $_2$, N $_2$ –CH $_4$, and CH $_4$ –CH $_4$ (Borysow & Frommhold 1986, 1987; Borysow & Tang 1993). The pressure broadening coefficient (γ_0) of HNC(6–5) was taken to be equal to that

of HCN(6–5), $\gamma_0 = 0.129$ cm $^{-1}$ bar $^{-1}$ at a reference temperature of 300 K and with a temperature dependency exponent $n = 0.69$ (Yang et al. 2008). The thermal profile used for our computation is a combination of (i) the temperatures measured by Huygens/HASI (Fulchignoni et al. 2005) in the troposphere at altitudes between 0–140 km; (ii) the disk-averaged Cassini/CIRS stratospheric temperatures (Vinatier et al. 2010) at altitudes between 140–500 km; (iii) the Cassini/INMS retrieved temperatures (i.e. 155 K in average, De La Haye et al. 2007) at altitudes between 1000–1500 km; (iv) a decreasing temperature from 165 K to 155 K at altitudes between 500 and 1000 km. Our modeling results, presented below, indicate that the HNC(6–5) line is optically thin (opacity $\tau \sim 0.12$), therefore results are not too sensitive to the precise temperature profile.

The model computes spectra in units of fluxes or Rayleigh-Jeans temperatures (T_{ij}). To compare T_{ij} with the measured antenna temperature (T_a), we use the usual relationship: $T_a = T_{ij}/F_d \times B_{\text{eff}}/F_{\text{eff}}$, with F_d the geometrical dilution factor, B_{eff} the telescope beam efficiency (i.e. 0.75), and F_{eff} the telescope forward efficiency (i.e. 0.96). Because the HRS spectra are much noisier (due to their higher spectral resolution) than the WBS data, we focussed on the WBS spectra, averaging the two epochs to further improve the S/N.

3.1. Uniform mixing ratio profiles

The HNC narrow linewidth indicates that the line is mostly Doppler-broadened, with little or no contribution from Lorentz linings. In a first series of models, we considered uniform vertical distributions of HNC, i.e. with a constant mixing ratio q_0 above a given altitude z_0 . In this approach, one can discard HNC profiles with z_0 smaller than 200 km, because the associated simulated lines are broader than the observed line (i.e. pressure-broadened, Fig. 2). While a value of z_0 equal to 300 km is still acceptable, we favor uniform profiles in which z_0 is greater than 400 km. This, in particular, is also consistent with HNC being restricted to the upper thermosphere (e.g. $z_0 = 1000$ km). For such uniform distributions characterized by z_0 , the probed altitudes mainly lie between z_0 and $z_0 + 100$ km. Best-fit results of the coupled parameters z_0 and q_0 are given in Table 2. The retrieved column density depends slightly on z_0 , and lies in the range $(0.6\text{--}1.5) \times 10^{13}$ cm $^{-2}$ for z_0 varying between 400 and 1000 km, with higher values of z_0 associated with smaller columns.

3.2. A thermospheric case

As illustrated above, our observations do not establish the vertical distribution of HNC, except for the loose constraint that it cannot be present in large amounts below 300 km. Nevertheless, as we discuss below, formation scenarios argue for a large fraction of HNC to be restricted to the thermosphere, with its distribution roughly following that of the electronic density in the lower ionosphere. To mimic this situation, we tested the case in which HNC is restricted to a layer from 900 to 1200 km, with a constant number density (i.e. a mixing ratio (q) increasing with altitude as $q = q_0 \times (p_0/p)$, with p_0 the reference pressure corresponding to $z_0 = 900$ km). For altitudes lower than z_0 , the mixing ratio is taken as zero. Taking into account the high molecular diffusion above the homopause at ~ 1200 km ($D = 0.5\text{--}1 \times 10^{10}$ cm 2 s $^{-1}$, De La Haye et al. 2007; Yelle et al. 2008), we also assumed a constant mixing ratio above the homopause $z_h = 1200$ km. With this model, the best fit is obtained

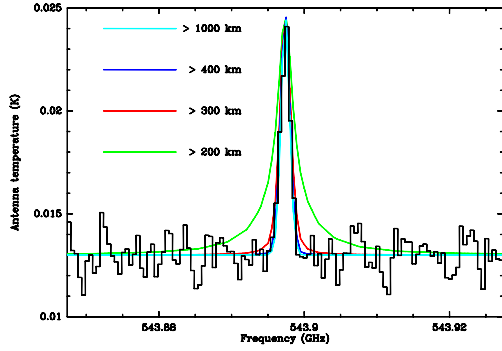
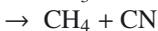


Fig. 2. Models of the HNC(6–5) line, assuming a uniform mixing ratio distribution of HNC above altitudes of 1000, 400, 300, and 200 km, corresponding to cases A, G, H, and I, respectively, in Table 2. These models are compared with the averaged WBS spectrum from June/Dec.

for $q_0(900 \text{ km}) = (2.0^{+0.4}_{-0.4}) \times 10^{-6}$. It corresponds to an HNC column density of $5.7^{+1.1}_{-1.1} \times 10^{12} \text{ cm}^{-2}$, close to the one retrieved for uniform A or B cases (Table 2). Extending this approach to other values of z_0 , we also computed models with increasing mixing ratio with altitude as $q = q_0 \times (p_0/p)^n$. Many possible fits were found for z_0 between 300–1000 km, further demonstrating that we cannot currently constrain the vertical distribution of HNC. The retrieved column density remains unchanged at $(0.6\text{--}1.5) \times 10^{13} \text{ cm}^{-2}$.

4. Discussion

The possible presence of HNC in Titan's atmosphere was first considered by Petrie (2001). Based on pre-Cassini photochemical models (e.g. Ip 1990; Galand et al. 1999; Banaszekiewicz et al. 2000) which predicted that HCNH^+ is one important or even the dominant ion at the ionospheric peak, Petrie (2001) postulates the dissociative recombination of HCNH^+ ($\text{HCNH}^+ + e^- \rightarrow \text{HNC} + \text{H}$) as an important source of HNC. This reaction, which produces HCN and HNC in approximately equal yields, was suggested as the origin of the high abundance of HNC ($\text{HNC} \sim \text{HCN}$) in dense molecular clouds as early as 35 years ago (Watson 1976). Petrie (2001) further considered various loss processes for HNC, including (i) photon-induced isomerization ($\text{HNC} + h\nu \rightarrow \text{HCN}$); (ii) photolysis ($\text{HNC} + h\nu \rightarrow \text{H} + \text{CN}$); (iii) H-catalyzed isomerization ($\text{HNC} + \text{H} \rightarrow \text{HCN} + \text{H}$); (iv) protonation with ionospheric cations ($\text{XH}^+ + \text{HNC} \rightarrow \text{X} + \text{HCNH}^+$); and (v) reactions with neutral radicals ($\text{X} + \text{HNC} \rightarrow \text{XCN} + \text{H}$ or $\text{XH} + \text{CN}$). He dismissed (i) and (ii) as being insignificant compared to protonation and retained the other three loss mechanisms, focussing on process (v) with $\text{X} = \text{CH}_3$. Using this limited chemistry, HNC would therefore result from the following sets of reactions:



The detection of HCNH^+ by INMS with a peak abundance of $\sim 10^3 \text{ cm}^{-3}$ near 1100–1150 km (e.g. Waite et al. 2005; Vuitton et al. 2007; Cui et al. 2009) supports the above production scheme and allows one to evaluate it quantitatively, although key reaction rates (k_i) are still uncertain. The dissociative recombination rate of HCNH^+ depends on the electron temperature. The

Table 2. Retrieved HNC mixing ratio and column density assuming uniform profiles above altitude z_0 .

Profile	$\geq z_0$ (km)	Mixing ratio	Column (cm^{-2})
A	1000	$6.0^{+1.5}_{-1.0} \times 10^{-5}$	6.3×10^{12}
B	900	$1.4^{+0.3}_{-0.3} \times 10^{-5}$	6.9×10^{12}
C	800	$3.1^{+0.8}_{-0.6} \times 10^{-6}$	7.8×10^{12}
D	700	$6.7^{+1.8}_{-1.2} \times 10^{-7}$	8.9×10^{12}
E	600	$1.3^{+0.3}_{-0.3} \times 10^{-7}$	1.0×10^{13}
F	500	$2.6^{+0.8}_{-0.5} \times 10^{-8}$	1.2×10^{13}
G	400	$4.5^{+1.2}_{-1.0} \times 10^{-9}$	1.5×10^{13}
H	300 ^a	$1.1^{+0.3}_{-0.3} \times 10^{-9}$	2.0×10^{13}
I	200 ^b	$0.4^{+0.1}_{-0.1} \times 10^{-9}$	–

Notes. Mixing ratio include uncertainties in HIFI calibration ($\sim 10\%$, Roelfsema et al. 2011) and statistical uncertainties. ^(a) Linewidth is marginally too large. ^(b) Linewidth is too large.

Cassini Radio and Plasma Wave Science (RPWS/LP) measurements have reported an electronic temperature of 500 K (Ågren et al. 2009; Galand et al. 2010) over 950–1100 km. Such a value is surprisingly high, because electronic temperatures closer to the $\sim 150 \text{ K}$ gas temperature are expected below $\sim 1050 \text{ km}$ (Richards et al. 2011). We therefore considered both $T_e = 150 \text{ K}$ and $T_e = 500 \text{ K}$, giving $k_{1a} = k_{1b} = 1.5 \times 10^{-7} \text{ cm}^3 \text{ s}^{-1}$ and $6.90 \times 10^{-8} \text{ cm}^3 \text{ s}^{-1}$, respectively (Semaniak et al. 2001).

As discussed by Petrie (2001), protonation is likely to involve virtually all hydrogen-bearing ions, so it is reasonable to adopt a total XH^+ concentration equal to the electron density. In particular, the $\text{HCNH}^+ + \text{HNC}$ reaction has been investigated theoretically, and suggested to be a significant loss channel for HNC in molecular clouds (Pichierri 2002). To our knowledge however, no measurements of the protonation rates for HNC are available. Petrie uses $k_2 = 3.5 \times 10^{-9} \text{ cm}^3 \text{ s}^{-1}$. The Su-Chesnavich formulae (see Woon & Herbst 2009) would give $k_2 = 5.2 \times 10^{-9} \text{ cm}^3 \text{ s}^{-1}$ at 150 K. As this value seems high compared to typical protonation rates (Vigren, priv. comm.), we here considered $k_2 = 3.5 \times 10^{-9} \text{ cm}^3 \text{ s}^{-1}$ and $k_2 = 1 \times 10^{-9} \text{ cm}^3 \text{ s}^{-1}$. With a peak electron density of $\sim 2000 \text{ cm}^{-3}$ (Wahlund et al. 2009), this gives a loss rate of $(2\text{--}7) \times 10^{-6} \text{ s}^{-1}$.

Following Talbi et al. (1996) we adopt a $k_3 = 1 \times 10^{-14} \text{ cm}^3 \text{ s}^{-1}$ reaction rate (at 150 K) for the H-catalyzed isomerization reaction (3). Based on various models (e.g. Lara et al. 1996; De La Haye et al. 2008), the [H] mixing ratio near 1100 km is in the range $(4\text{--}10) \times 10^{-4}$. Adopting 4×10^{-4} from De La Haye et al. (2008), which gives [H] $\sim 1.3 \times 10^6 \text{ cm}^{-3}$ at 1100 km, implies a loss rate of $\sim 1.3 \times 10^{-8} \text{ s}^{-1}$ through reaction (3), much lower than the above losses from ion-neutral reactions. Regarding the $\text{CH}_3 + \text{HNC}$ (4) reaction rate, Petrie (2001) considered two extreme values ($k_4 = 10^{-14}$ and $k_4 = 5 \times 10^{-11} \text{ cm}^3 \text{ s}^{-1}$), but in a more recent study, Petrie & Osamura (2004) indicate a much lower rate ($9.2 \times 10^{-20} \text{ cm}^3 \text{ s}^{-1}$ at 200 K). With this value and a CH_3 concentration of $\sim 2 \times 10^6 \text{ cm}^{-3}$ at 1100 km (e.g. Hörst et al. 2008), the associated loss is entirely insignificant, and the HNC abundance is thus controlled by reactions (1a) and (2).

With the above scenario, the chemical lifetime of HNC is $(1.4\text{--}5) \times 10^5 \text{ s}$, i.e. 3 to 10 times shorter than Titan's day and comparable to the day-to-night transport time (about $2 \times 10^5 \text{ s}$ for $\sim 50 \text{ m/s}$ thermospheric winds, Müller-Wodarg et al. 2008). HCNH^+ shows strong diurnal variations with maximum (day-side) concentrations of $\sim 1000 \text{ cm}^{-3}$ at 1000–1200 km (Cui et al. 2009), and about five times less on the nightside, implying that (unobservable so far) diurnal variations of HNC can be expected. The HNC chemical lifetime is comparable to the

transport timescale (1.5×10^5 s at 1000 km, for a $\sim 3 \times 10^8$ cm² s⁻¹ diffusion coefficient, Yelle et al. 2008) As a result, HNC in the ionosphere is affected by both chemical and transport losses, but its distribution may be reasonably close to photochemical equilibrium. In this framework, and considering only the protonation loss with $[XH^+] = [e^-]$, the HNC concentration can be simply written as $[HNC] = k_{1a}/k_2 \times [HCNH^+]$, where the equality holds either for concentrations or column densities. With an HCNH⁺ dayside (relevant for our purpose) column density of 3.5×10^{10} cm⁻², and using each of these two values considered for k_{1a} and for k_2 , we obtain an HNC column of 7×10^{11} – 5.2×10^{12} cm⁻². The upper range is consistent with the measurements, although somewhat marginally.

The above calculations only consider HNC production from HCNH⁺, while any other ion that includes the -CNH⁺ group may lead to HNC upon recombination. HCNH⁺ is the dominant ion measured by INMS, followed by C₂H₅⁺, HC₃NH⁺, c-C₃H₃⁺, C₃H₅⁺ (Cui et al. 2009), but RPWS and the Cassini Plasma Spectrometer (CAPS) measurements indicate that heavy ions beyond the mass range of INMS (>100 amu) contribute significantly, constituting $\sim 5\%$ of the ionosphere near 1100 km and becoming even dominant (50–70 %) over 950–1000 km altitude (Crary et al. 2009; Wahlund et al. 2009). Nitrile ions heavier than HCNH⁺ have higher recombination rates, e.g. by factors 3 to 5 for HC₃NH⁺ and other species measured by Vigren et al. (2011). Remarkably, “effective” recombination rates for Titan’s ionosphere, based on CAPS and RPWS/LP measurements (Galand et al. 2010), increase below 1200 km, reaching $\sim 5 \times 10^{-6}$ cm³ s⁻¹ at 1000 km, a behavior attributed to the change of composition below the ionospheric peak and the progressive onset of heavy ions. Since heavy nitrile ions in this altitude range could provide significant additional sources of HNC, we conclude that a purely ionospheric source may be quantitatively viable for HNC, provided the protonation rates are not too high.

Even if a primarily ionospheric production is assumed, HNC will not necessarily be restricted to the ionosphere, as it must be transported downward to some extent by eddy mixing. This will further increase its chemical lifetime, in relation to the decline of ion-molecule reactions. Petrie & Osamura (2004) find that in the neutral atmosphere, H-catalyzed isomerization (3) may be the main loss channel for HNC, with additional contributions from reactions with CN and C₃N. Photolysis and photo-isomerization of HNC, albeit negligible at ionospheric levels, must also become significant there, especially the latter, which has a very low energy threshold (8510 Å, see Petrie 2001). Additional formation routes to HNC in the neutral atmosphere should also be investigated, in particular its production through N(⁴S) + ³CH₂. This pathway produces equal amounts of HCN and HNC and has been invoked in the regulation of the HNC/HCN abundance in molecular clouds (Herbst et al. 2000). We leave these issues for future photochemical modeling, with the goal of matching HNC and HCN simultaneously. We note that, in the model where HNC is restricted to altitudes above 1000 km, its mole fraction is $\sim 6 \times 10^{-5}$. Comparing with the HCN abundance from INMS (2.0×10^{-4} , Vuitton et al. 2007) indicates HNC/HCN ~ 0.3 ; thus, a significant contribution of HNC to the mass 27 signal is likely.

In the Solar System, HNC has been observed in many comets since its first discovery in comet Hyakutake, with HNC/HCN abundance ratios varying from $\leq 2\%$ to 20% (Irvine et al. 1996; Lis et al. 2008). The inverse correlation of this ratio with heliocentric distance argues for the production of HNC from the thermal degradation of organic grains heated by the Sun (Lis et al. 2008). A production of HNC from solid (haze) material in Titan’s atmosphere might therefore not be excluded, although

this remains largely speculative. In this respect, and more generally to constrain photochemical models, determining the vertical profile of HNC and its abundance in the region of the main haze (300–500 km) would be important. Although observing other (and stronger) additional lines of HNC might help slightly, this will probably require limb observations from a Titan orbiter equipped with a submillimeter instrument (Lellouch et al. 2010).

Acknowledgements. HIFI has been designed and built by a consortium of institutes and university departments from across Europe, Canada, and the United States under the leadership of SRON Netherlands Institute for Space Research, Groningen, The Netherlands, and with major contributions from Germany, France, and the US. We acknowledge very useful discussions with M. Galand, E. Vigren, E. Herbst, S. Petrie and O. Dutuit. L.M. Lara’s work has been supported by the Ministry of Innovation and Science through the project AyA 2009-08011.

References

- Ågren, K., Wahlund, J.-E., Garnier, P., et al. 2009, *Planet. Space Sci.*, 57, 1821
 Banaszekiewicz, M., Lara, L. M., Rodrigo, R., López-Moreno, J. J., & Molina-Cuberos, G. J. 2000, *Icarus*, 147, 386
 Borysow, A., & Frommhold, L. 1986, *ApJ*, 311, 1043
 Borysow, A., & Frommhold, L. 1987, *ApJ*, 318, 940
 Borysow, A., & Tang, C. 1993, *Icarus*, 105, 175
 Crary, F. J., Magee, B. A., Mandt, K., et al. 2009, *Planet. Space Sci.*, 57, 1847
 Cui, J., Galand, M., Yelle, R. V., et al. 2009, *J. Geophys. Res.*, A, 114, A06310
 de Graauw, T., Helmich, F. P., Phillips, T. G., et al. 2010, *A&A*, 518, L6
 De La Haye, V., Waite, J. H., Johnson, R. E., et al. 2007, *J. Geophys. Res.* A, 112, A07309
 De La Haye, V., Waite, J. H., Cravens, T. E., Robertson, I. P., & Lebonnois, S. 2008, *Icarus*, 197, 110
 Fulchignoni, M., Ferri, F., Angrilli, F., et al. 2005, *Nature*, 438, 785
 Galand, M., Liliensten, J., Toublanc, D., & Maurice, S. 1999, *Icarus*, 140, 92
 Galand, M., Yelle, R., Cui, J., et al. 2010, *J. Geophys. Res.* A, 115, A07312
 Gurwell, M. A. 2004, *ApJ*, 616, L7
 Gurwell, M. A., & Muhleman, D. O. 1995, *Icarus*, 117, 375
 Hartogh, P., Lellouch, E., Crovisier, J., et al. 2009, *Planet. Space Sci.*, 57, 1596
 Herbst, E., Terzieva, R., & Talbi, D. 2000, *MNRAS*, 311, 869
 Hidayat, T., Marten, A., Bezard, B., et al. 1998, *Icarus*, 133, 109
 Hörst, S. M., Vuitton, V., & Yelle, R. V. 2008, *J. Geophys. Res.*, E, 113, E10006
 Ip, W.-H. 1990, *ApJ*, 362, 354
 Irvine, W. M., Bockelee-Morvan, D., Lis, D. C., et al. 1996, *Nature*, 383, 418
 Lara, L. M., Lellouch, E., López-Moreno, J. J., & Rodrigo, R. 1996, *J. Geophys. Res.*, E, 101, 23261
 Lellouch, E., Vinatier, S., Moreno, R., et al. 2010, *Planet. Space Sci.*, 58, 1724
 Lis, D. C., Bockelee-Morvan, D., Boissier, J., et al. 2008, *ApJ*, 675, 931
 Marten, A., Hidayat, T., Biraud, Y., & Moreno, R. 2002, *Icarus*, 158, 532
 Moreno, R., Marten, A., & Hidayat, T. 2005, *A&A*, 437, 319
 Müller-Wodarg, I. C. F., Yelle, R. V., Cui, J., & Waite, J. H. 2008, *J. Geophys. Res. (Planets)*, 113, 10005
 Ott, S. 2010, in *Astronomical Data Analysis Software and Systems XIX*, ed. Y. Mizumoto, K.-I. Morita, & M. Ohishi, ASP Conf. Ser., 434, 139
 Petrie, S. 2001, *Icarus*, 151, 196
 Petrie, S., & Osamura, Y. 2004, *J. Chem. Phys.* A, 108, 3623
 Pickett, H. M., Poynter, R. L., Cohen, E. A., et al. 1998, *J. Quant. Spec. Radiat. Transf.*, 60, 883
 Pilbratt, G. L., Riedinger, J. R., Passvogel, T., et al. 2010, *A&A*, 518, L1
 Rengel, M., Sagawa, H., & Hartogh, P. 2011, in *World Scientific, Singapore*, ed. A. Bhardwaj, *Adv. Geosci.*, 25, 173
 Richards, M. S., Cravens, T. E., Robertson, I., et al. 2011, *J. Geophys. Res.* A, in press
 Roelfsema, P. R., Helmich, F. P., Teysier, D., et al. 2011, *A&A*, in press, DOI: 10.1051/0004-6361/201015120
 Semaniak, J., Minaev, B. F., Derkach, A. M., et al. 2001, *ApJS*, 135, 275
 Talbi, D., Ellinger, Y., & Herbst, E. 1996, *A&A*, 314, 688
 Vigren, E., Semaniak, J., Hamberg, M., et al. 2011, *Planet. Space Sci.*, in press
 Vinatier, S., Bézard, B., Nixon, C. A., et al. 2010, *Icarus*, 205, 559
 Vuitton, V., Yelle, R. V., & McEwan, M. J. 2007, *Icarus*, 191, 722
 Wahlund, J.-E., Galand, M., Müller-Wodarg, I., et al. 2009, *Planet. Space Sci.*, 57, 1857
 Waite, J. H., Niemann, H., Yelle, R. V., et al. 2005, *Science*, 308, 982
 Watson, W. D. 1976, *Rev. Mod. Phys.*, 48, 513
 Woon, D. E., & Herbst, E. 2009, *ApJS*, 185, 273
 Yang, C., Buldyreva, J., Gordon, I. E., et al. 2008, *J. Quant. Spec. Radiat. Transf.*, 109, 2857
 Yelle, R. V., Cui, J., & Müller-Wodarg, I. C. F. 2008, *J. Geophys. Res.* E, 113, E10003